II. RADIO ASTRONOMY

Academic and Research Staff

Prof. A. H. Barrett
Prof. B. F. Burke
Prof. Susan G. Kleinmann
Prof. R. M. Price
Prof. D. H. Staelin
Dr. P. L. Kebabian
Dr. K. F. Kunzi
Dr. P. C. Myers
Dr. G. D. Papadopoulos
Dr. J. Sander
Dr. J. W. Waters
J. W. Barrett
D. C. Papa

Graduate Students

B. G. Anderson
O. Appiah
K. P. Bechis
W. G. Brodsky
P. C. Crane
R. W. Freund
T. S. Giuffrida
A. D. Haschick
P. Ho
K-S. Lam
S. Lee
K-Y. Lo
R. N. Martin
R. W. McGahan
R. L. Pettyjohn
R. K. L. Poon
J. H. Spencer
R. C. Walker
T. J. Warren
R. W. Wilcox

A. INTERFEROMETRIC SURVEY OF THE RADIO EMISSION OF NORMAL GALAXIES

National Science Foundation (Grant GP-21348A#2)

P. C. Crane, R. M. Price

1. Introduction

We have initiated a high-resolution survey of the radio continuum emission of normal spiral and irregular galaxies. We plan to extend the survey to include a complete sample of such galaxies listed in the Reference Catalogue of Bright Galaxies[1] which are north of declination -20°, have angular sizes larger than 2-3 minutes of arc, and are brighter than magnitude 12.0. In radio source detections, we shall determine what classes of radio emission are present (for example, core only, core-hole, etc.) and their distribution according to morphological type.

Such a survey will represent considerable improvement over previous studies. The present survey will furnish a complete sample, whereas previous observations have been very selective. In the observations, by choice of frequency and angular resolution, we shall be able to detect the more variegated emission associated with galactic nuclei. In previous high-frequency observations generally the angular resolution has not been high enough to investigate such sources adequately.

2. Observations

In March 1973 we observed 185 spiral and irregular galaxies using the three-element dual-frequency interferometer of the National Radio Astronomy Observatory.[2] Our baselines of 300, 1200, and 1500 m give fringe spacings of up to 14."8 and 4."9 at our observing frequencies of 2695 MHz (11.1 cm) and 8085 MHz (3.7 cm), respectively. We observed each galaxy for two 25-min periods at complementary hour angles. Consequently, for a point source we had a 5σ detection level of 20 m.f.u. (1 m.f.u. = 10^{-29} W m^{-2} Hz^{-1}).

3. Data Reduction

The data were reduced according to the standard N.R.A.O. reduction programs.[2,3] Because of the limited hour-angle coverage and relatively short integration times, the maps thus obtained give only a rough indication of the characteristics of the sources. We are now using a new program (point-source model) to find the positions and fluxes of sources in our fields of view.

4. Results

The preliminary results indicate that 61 of the 185 observed galaxies have associated radio emission above the 20 m.f.u. level. It is important to remember that until we obtain accurate positions of our detected radio sources which can be compared with published optical positions[4,5] (accuracies $\leq 5''$), our identifications must be considered tentative.

We have also compared our observing list with lists of galaxies with peculiar nuclei published by J. L. Sersic.[6-8] Our list includes 17 of the 68 galaxies in these lists, comprising a more or less representative, but limited, selection. We have detections in the fields of 11 of these sources. The sample is not yet large enough nor are our results definite enough to provide conclusive correlations of radio properties with the types of optical peculiarity.

References

1. G. and A. de Vaucouleurs, Reference Catalogue of Bright Galaxies (University of Texas Press, Austin, Texas, 1964).
2. R. M. Hjellming, "An Introduction to the N.R.A.O. Interferometer," National Radio Astronomy Observatory, 1973.
3. B. Balick and E. Fomalont, "New Mapping System for the N.R.A.O. Dual Frequency Interferometer: A Preliminary Description," National Radio Astronomy Observatory, 1973.
4. L. Gallouet and N. Heidmann, Astron. Astrophys. Suppl. 3, 325 (1971).
5. L. Gallouet, N. Heidmann, and F. Dampierre (Astron. Astrophys. Suppl., in press).
6. J. L. Sersic and M. Pastoriza, Pub. Astron. Soc. Pacif. 77, 287 (1965).
7. J. L. Sersic and M. Pastoriza, Pub. Astron. Soc. Pacif. 79, 152 (1967).
8. J. L. Sersic, Pub. Astron. Soc. Pacif. 85, 103 (1973).

B. FURTHER RESULTS FROM THE NIMBUS-5 MICROWAVE SPECTROMETER EXPERIMENT

California Institute of Technology (Contract 952568)

D. H. Staelin, K. F. Kunzi, R. L. Pettyjohn, R. K. L. Poon, W. L. Smith, J. W. Waters, R. W. Wilcox

[W. L. Smith is with the National Oceanic and Atmospheric Administration.]

Preliminary evaluation of the data from the Nimbus-5 Microwave Spectrometer Experiment (NEMS) continues.[1,2]

One of the primary purposes of the experiment was to determine the ability of a passive microwave sounder to yield temperature profiles in the presence of clouds, and to compare this ability with that of infrared sounders.

The insensitivity of the NEMS temperature sounding channels to clouds is illustrated in Fig. II-1, where the relative brightness temperatures are plotted on an expanded

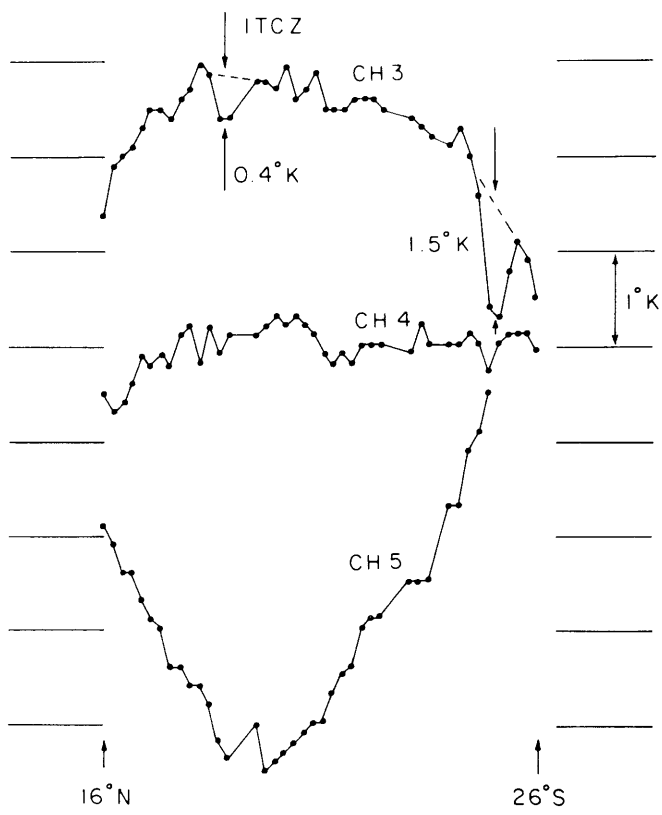

Fig. II-1. Relative brightness temperatures observed during orbit 163 as the satellite passed from 16° North to 26° South over the intertropical convergence zone (ITCZ).

scale for orbit 163 as the satellite crossed over the intertropical convergence zone (ITCZ). Even Channel 3, which senses near altitude 4 km, is largely unaffected by the substantial cloud development and precipitation that characterize the ITCZ. The largest deflections, 0.4°K and 1.5°K, are quite modest and of limited spatial extent. Channels 4 and 5 sense the atmosphere near 11 and 18 km, respectively, and show no effects of clouds anywhere.

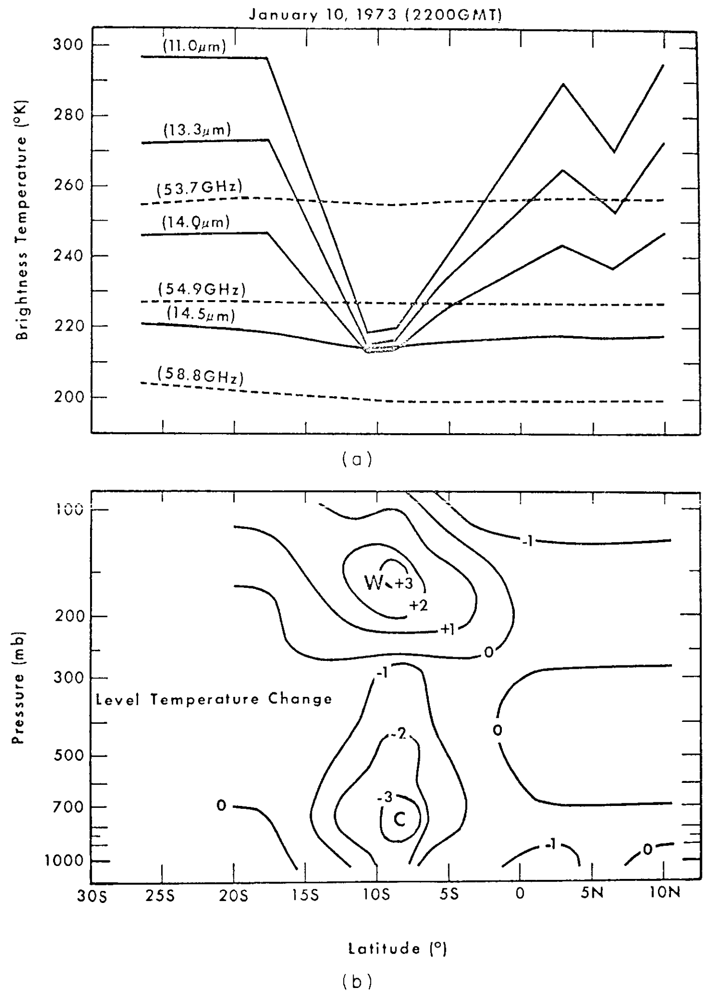

Fig. II-2. (a) Brightness temperatures observed by NEMS (microwave) and ITPR (infrared) channels over a tropical storm in the South Pacific on January 10, 1973. (b) Differences between temperature profiles inferred within the storm and those inferred outside the storm.

Figure II-2 shows the brightness temperature deflections[3] of the Infrared Temperature Profile Radiometer (ITPR) as it passed over the ITCZ on January 10, 1973. The NEMS data are presented for comparison, and are clearly less sensitive to such clouds.

In the bottom portion of the figure is the difference at each level between the atmospheric temperatures obtained within the storm and those obtained at the storm's boundary. Under the assumption that no actual variation in temperature profile exists, then the largest error incurred for these extreme cloud conditions is only 3.5°K. The possibility that the temperature profile varies across the storm as indicated by NEMS has not yet been excluded.

Figure II-3 is a map of the thickness of the 500-250 mb layer of the atmosphere.

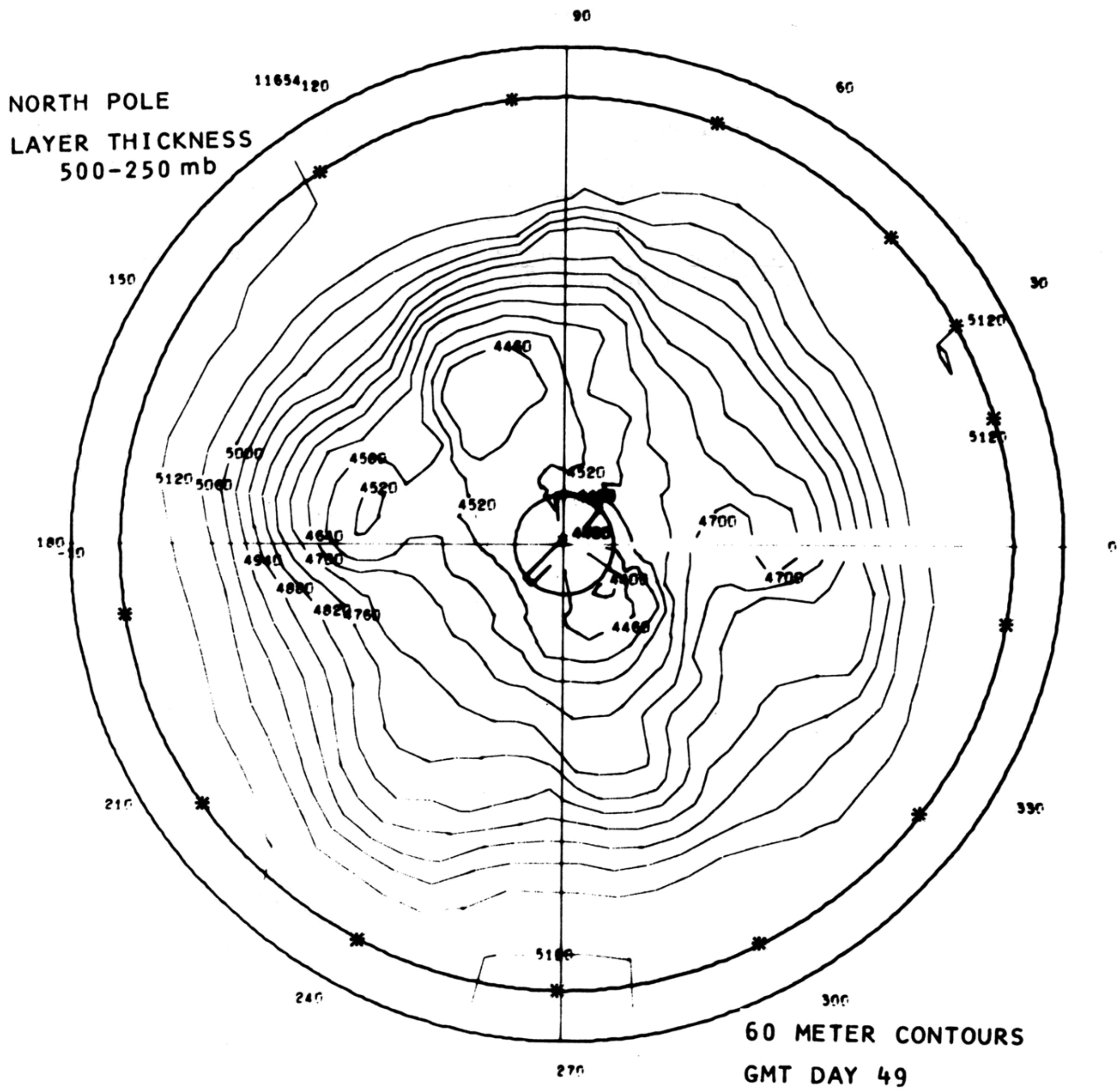

Fig. II-3. Thickness of the 500-250 mb atmospheric layer for the northern hemisphere, GMT day 49, 1973. Stars on equator mark ascending nodes of orbits incorporated in the map.

This map was obtained from NEMS data alone on GMT day 49, 1973, for the northern hemisphere. The contours are spaced at 60-m intervals, which approximately correspond to 3°K intervals in the average layer temperature. Despite the fact that NEMS views only the nadir, the map contains the major meteorological features present that day. Some weather features are not evident on this map because they were outside the nadir zones viewed by NEMS, a flaw that should be remedied by the scanning microwave spectrometer scheduled to provide global coverage in 1974. This map gives further evidence of the full coverage potential of microwave temperature sounders.

References

1. D. H. Staelin et al., Nimbus-5 User's Guide, Goddard Spaceflight Center, National Aeronautics and Space Administration, 1972, pp. 141-157.
2. D. H. Staelin et al., Quarterly Progress Report No. 109, Research Laboratory of Electronics, M.I.T., April 15, 1973, pp. 6-10.
3. W. L. Smith et al., Nimbus-5 User's Guide, Goddard Spaceflight Center, National Aeronautics and Space Administration, 1972, pp. 107-130.

C. MICROWAVE EMISSION FROM ATMOSPHERIC OXYGEN

National Aeronautics and Space Administration (Grant NGR 22-009-421)
U. S. Air Force – Electronic Systems Division (Contract F19628-73-C-0196)

A. H. Barrett, J. W. Barrett, K-S. Lam, D. C. Papa

A series of high-altitude balloon flights to measure microwave emission from atmospheric molecular oxygen was begun several years ago in order to compare microwave and infrared methods of determining atmospheric temperature profiles. The infrared portion of the experiment, which was to have been built by others, was subsequently canceled for lack of funds. Thus the microwave experiment was changed to conform to the Nimbus-E experiment and was planned to (i) test inversion procedures, (ii) fly the payload in a U-2 aircraft to sample a wide range of weather phenomena, and (iii) provide data from which theoretical microwave line profiles could be checked.

Flights were conducted during the period 1963-1968 and have been reported previously. The present experiments were carried out with a completely new payload incorporating solid-state components, with the result that we now have a lighter, more sensitive, payload.

1. Radiometer

The microwave section of the radiometer is basically the same as in the radiometer flown in the past. The post-detection section is of a new design, as is the data-recording section.

A block diagram of the basic balloon-borne system is shown in Fig. II-4. The main improvement over our past O_2 single-channel radiometer is the use of a channel-dropping filter that splits the RF signal into two different radiometers while the remaining unfiltered signal is fed into the third radiometer. This configuration allows the use of only one antenna for the entire system and permits common calibration temperatures for the three channels. Figure II-5 shows typical losses for the filter system. Other improvements are a change from power-consuming klystrons to Gunn oscillators for the local-oscillator signals and modifications in the design of the low-noise mixer preamplifiers. The Gunn oscillators enable operation of 3 local oscillators with a total power consumption of 4.5 W, whereas in the past a single klystron and power supply consumed nearly 30 W.

The mixers were developed in-house at the Research Laboratory of Electronics with assistance from R. W. Chick at Lincoln Laboratory, M.I.T. We were able to obtain a limited number of diodes from Mr. Chick which gave mixers with noise figures of 6.5-8.8 dB. We were not able to have them more nearly equal because we lacked sufficient diode pairs to get the best match.

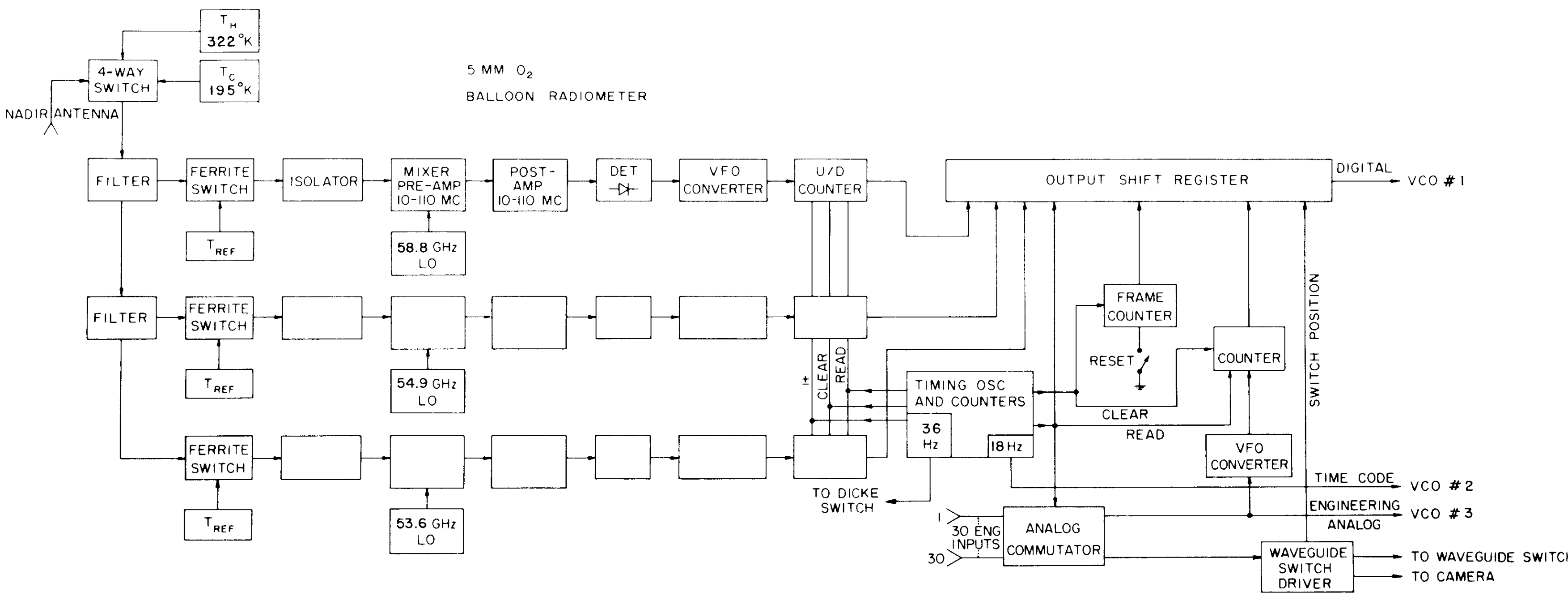

Fig. II-4. Radiometer block diagram.

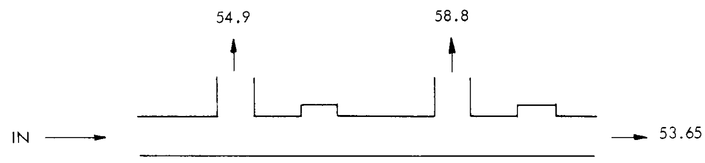

FREQUENCY (GHz)	LOSS (dB)
53.65	0.9
54.90	2.1
58.80	2.0

Fig. II-5. Channel-dropping filter.

When the entire system was assembled additional losses were introduced by the channel-dropping filters and the mechanical switch and feed horn assembly.

By interchanging mixers to achieve the most balanced system, we obtained system noise figures of 8.2 dB at 53.6 GHz, 9.7 dB at 54.9 GHz, and 9.9 dB at 58.8 GHz. The mixers were followed by an IF system with 75-dB gain and 10-110 MHz bandwidth.

The high-temperature calibration is performed with a waveguide termination around which an electrical heater is wound. Two thermistors are imbedded in the load material. One is part of a bridge circuit to control the heating element, the other is part of the temperature monitoring system. The temperature is set at 48°C.

The low-temperature calibration is performed with a waveguide termination immersed in a dewar filled with a mixture of alcohol and dry ice. A thermistor is imbedded in the load material and connected to a temperature-monitoring system. The entire dewar is pressurized during flight with a constant-pressure valve system. The bath temperature is -78°C.

The video detector is followed by a dc amplifier which allows for gain adjustments into the digital system.

The operation of the entire payload is controlled by an on-board digital synchronous detector and control system. The basic oscillator operates at 9.2 kHz and is divided down to provide all control signals, such as the Dicke switching frequency, the read and clear pulses, the clock frequency, waveguide switch control, and the camera commands.

The basic integration period is 4 s during which the radiometer signal is fed into the up/down counters and allowed to accumulate. At the end of the 4-s period the contents is fed to a shift register to be read out during the next 4-s cycle. The up/down counters are 16-bit counters; 12 of the most significant bits are fed to the shift register. The length of the entire shift register is 72 bits which allows 12 bits for each of the three radiometer channels, 12 bits for the frame counter, 12 bits for engineering data, 3 bits for the mechanical switch position, and 9 bits for a built-in "sync" word.

The timing is such that we begin with a 20-s low-temperature calibration

(5 integration periods), a 20-s high-temperature calibration, and 320 s of atmospheric emission observations.

The entire digital system is constructed of new low-power C/MOS digital logic. The power consumption is less than 10 mW total at 5 V. Again, this is a great saving over the power that would be required from a battery using regular TTL or DTL logic.

The contents of the shift register, which contains all of the flight information, is fed to an on-board digital recorder, which serves as a data back-up should we encounter telemetry problems, and also to one of the three VCO channels for transmission to the ground. The clock is sent to another VCO channel to the ground station. An analog display of our "housekeeping" commutator is also telemetered to enable us to monitor the system during flight.

2. Balloon Flights

Two flights were scheduled at the National Center for Atmospheric Research (NCAR), in Palestine, Texas. The first flight took place on March 27, 1973 and the second on April 2, 1973. Both flights were planned for roughly the same flight profile: sunrise launch, ascent at ~1000 ft/min to a float altitude of ~100,000 ft, float for ~2 h, a valve-down descent at ~200-300 ft/min to ~15,000 ft, then parachute descent to ground. The entire duration of each flight was to be ~8 h (Fig. II-6). The flight paths were easterly because of prevailing wind conditions.

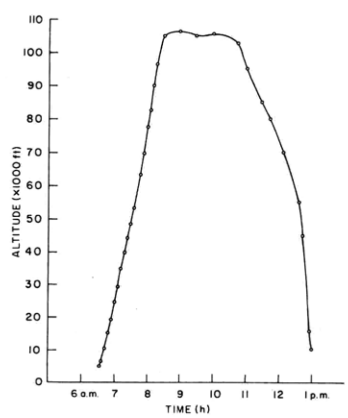

Fig. II-6. Flight profile F737P.

The principal block in our data format is a cycle furnishing six minutes worth of data. The main data contents is the following.

(i) Frame numbers, used for correlating data with time.

(ii) Engineering (housekeeping) data – monitored temperatures and voltages at various locations of the gondola.

(iii) Microwave data – cold calibration (~ −78.5°C), hot calibration (~48°C), and antenna temperatures for the three radiometer channels.

Data were recorded on board by a digital cassette write recorder (Memodyne model No. 201) for the duration of the experiment and also received on ground through telemetry, first at the base in Palestine, and then at the downrange station in Laurel, Mississippi, toward the end of the flight. A complete record of the telemetered data was made both on punched paper and magnetic tapes. An HP printer and PDP 11/20 8k memory computer at NCAR provided the capability of looking at data on a real-time basis when desired. The on-board cassette tape was played back on a read recorder (Memodyne model No. 102) after recovery and interfaced into the PDP-11 computer. Programs have been constructed to look at raw data and reduced data (giving the antenna temperatures and the ΔT_{rms}). The engineering data were also displayed through stripchart recorders at Palestine, Texas, and at Laurel, Mississippi.

On the morning of March 27, 1973, NCAR Flight No. 737P was launched at 6:30 a.m. The system ascended smoothly at an average rate of 875 ft/min to ~105,000 ft, reaching that altitude at ~8:30 a.m. At about the same time, the computer graphical output of

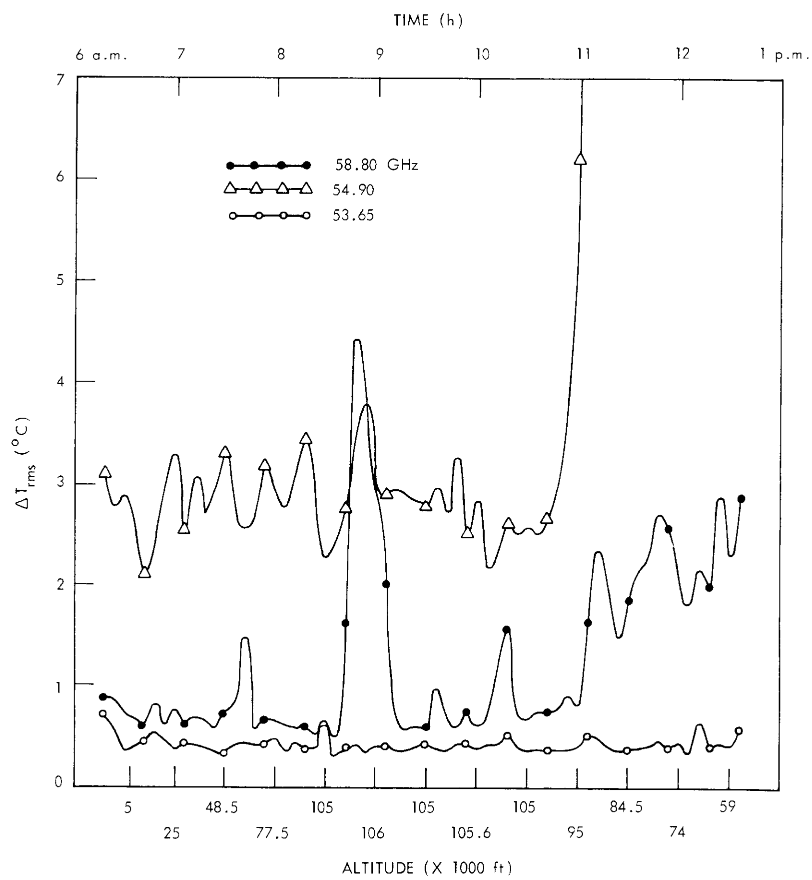

Fig. II-7. ΔT_{rms} for F737P.

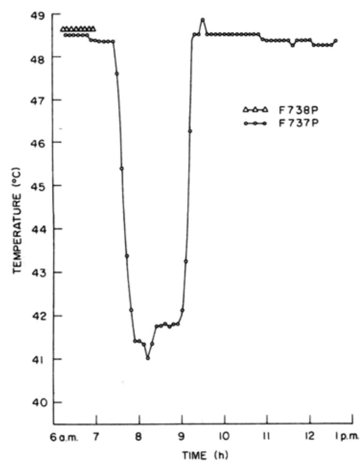

Fig. II-8. Hot load temperature profile.

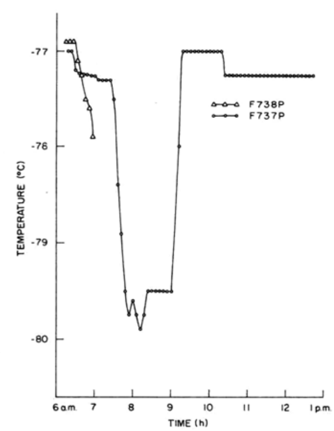

Fig. II-9. Cold load temperature profile.

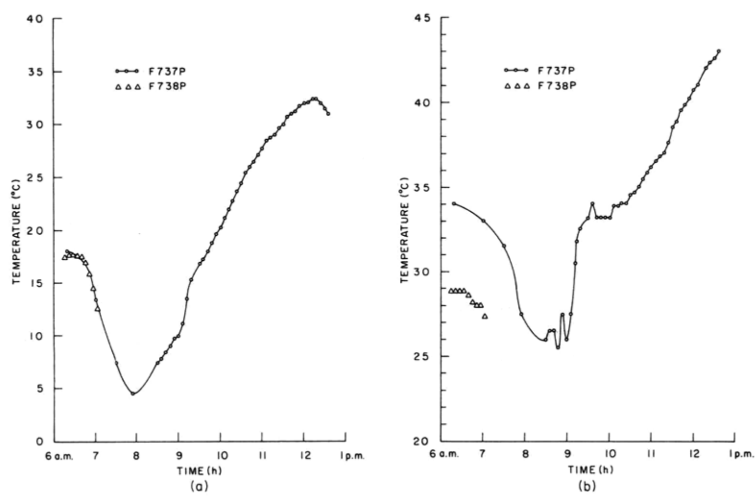

Fig. II-10. Temperature profile for (a) gondola, (b) radiometer box.

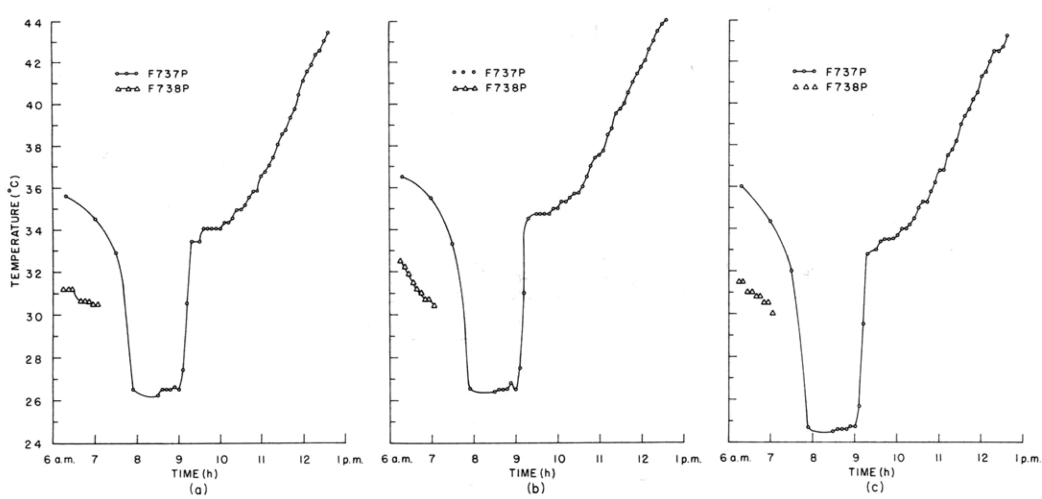

Fig. II-11. Ferrite switch temperature profile. (a) 53.65 GHz, (b) 54.9 GHz, (c) 58.8 GHz.

data was lost because of software problems on the ground. The gondola stayed at float altitude for ~2 h, and the valve-down process started at 10:30 a.m. at an average rate of ~350 ft/min. At ~11 a.m. it was noticed through the HP printer output that the 54.9 GHz channel was becoming noisy. The ΔT_{rms} climbed from ~3° to ~13° in 30 min (see Fig. II-7). Consequently, the ΔT_{rms} for this channel stayed at a value of 15° and did not return to its normal ~3° during the whole flight. The 58.8 GHz channel also started to deteriorate by 11 a.m. as its ΔT_{rms} suffered an increase of ~1.6° in 30 min. The 53.65 GHz channel, however, retained its normal performance. At 12:30 p.m. (package at altitude 60,000 ft) the balloon developed a serious defect and the system started to descend at an uncontrollable rate. The balloon was cut loose and the gondola descended on parachute. The impact occurred at 1:12 p.m., near Carthage, Mississippi. The gondola was recovered shortly afterwards and shipped back to Palestine, Texas, on the following day.

For this flight, radiosonde data of temperature and relative humidity vs pressure altitude were taken at Palestine, Texas, Shreveport, Louisiana, and Jackson, Mississippi.

The package suffered no external injuries, except for a slightly dented horn. The radiometers had reverted to their normal performance. From the engineering data (see Figs. II-8 through II-11) we deduced that on the ascent the gondola box was quite sensitive to the temperature drop of the environment. The main problem, however, was that during the float portion of the flight, the package absorbed excessive solar heat. This was enhanced by the fact that dark-green tape was put over three-quarters of the external surface of the package. The net result was that the interior of the radiometer box reached a temperature of 50°C. We suspect that the excessive heat affected the performance of the ferrite switches.

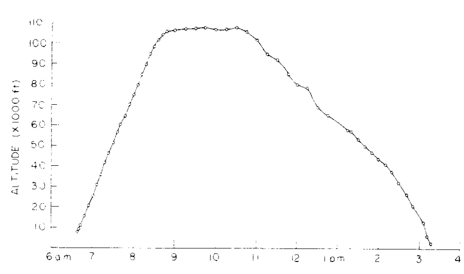

Fig. II-12. Flight profile F738P.

The following steps were taken to remedy the thermal problem:

1. Some foam insulation was removed.

2. The heater circuit in the radiometer box was adjusted to operate at a lower temperature.

3. Aluminum foil was packed between the radiometer box and the gondola box to provide for better heat conduction.

4. White tape was put on the exterior to increase the reflection of the sunlight.

The beacon transmitter used for flight control was found to have a noticeable effect on the 58.8 GHz channel. When it was activated the ΔT_{rms} suffered an increase of ~3°K.

The recovered cassette tape was played back through the PDP-11 computer during the entire flight. Only one bad frame, in a total of 6020 recorded, was noted.

The second flight profile, F738P (Fig. II-12) was essentially the same as that of F737P, except that the valve-down proceeded to its completion at 15,000 ft. Impact occurred at 3:10 p.m., near Tuscaloosa, Alabama. The package was recovered and returned to Palestine, Texas, on April 4, 1973 in excellent condition. For this flight

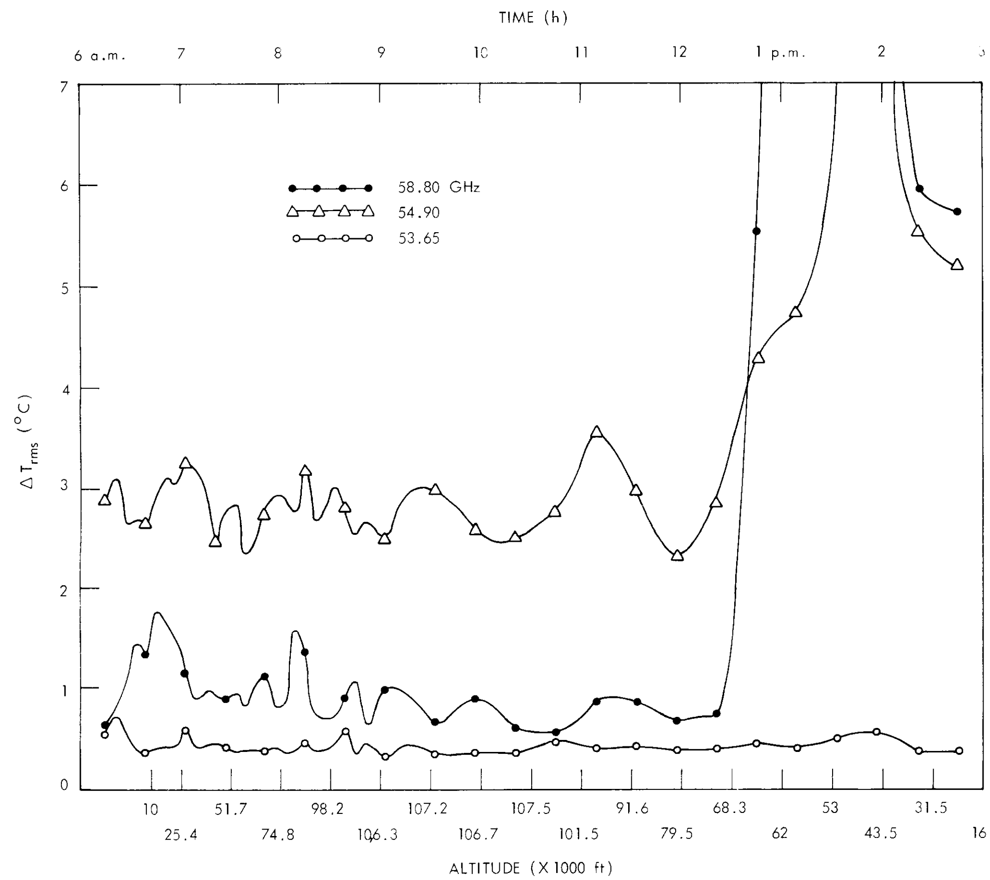

Fig. II-13. ΔT_{rms} for F738P.

both the 58.8 GHz and the 54.9 GHz channels were observed to deteriorate starting at 12:30 p.m., the ΔT_{rms} increasing from ~0.6° to ~10° (see Fig. II-13) and from ~3° to ~10°, respectively. The complete loss of the engineering data after 7:10 a.m. precluded

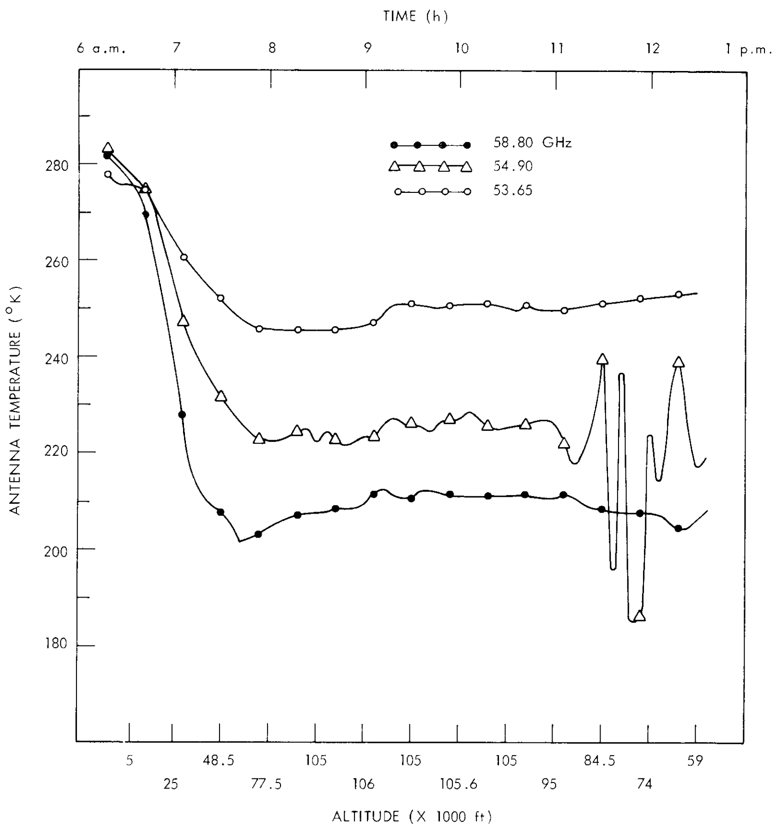

Figure II-14.
Antenna temperature profile F737P.

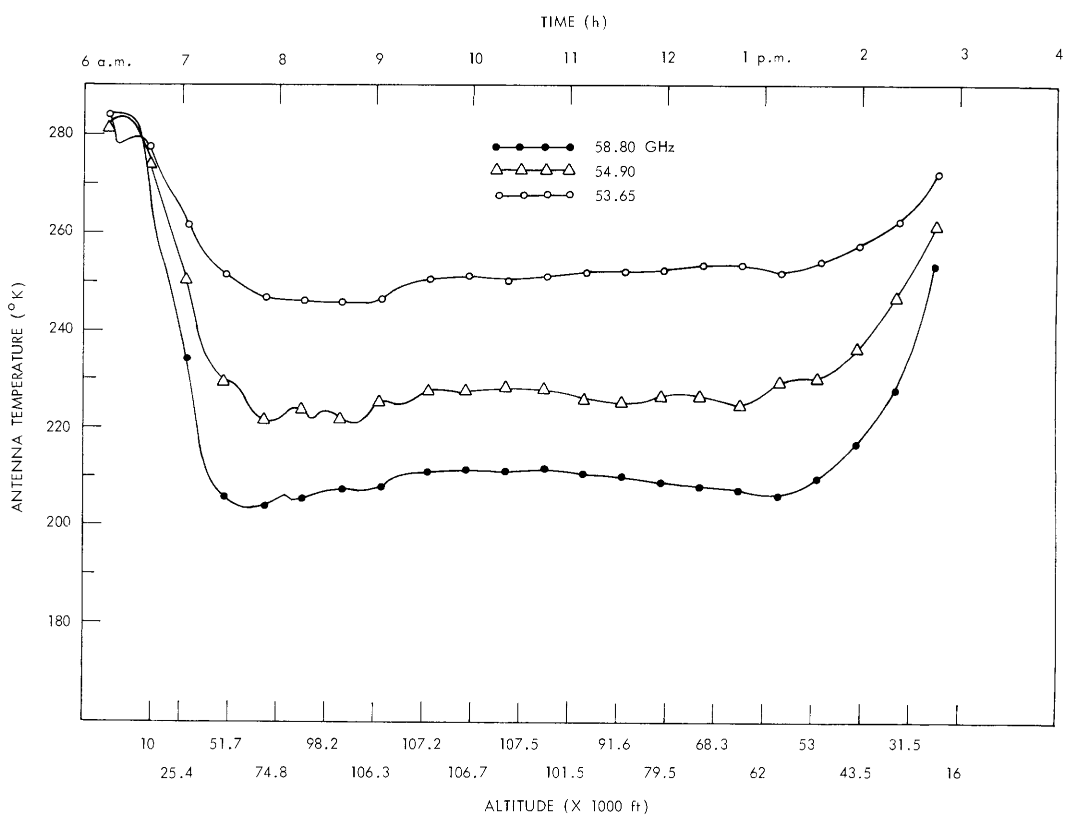

Fig. II-15. Antenna temperature profile F738P.

a meaningful examination of the experimental thermal conditions in the package.

A different cassette tape was used for on-board recording for this flight and on playback the error rate was found to be 4 frames in 8010.

Radiosonde data for this flight were taken at Palestine, Texas, Shreveport, Louisiana, Jackson, Mississippi, and Montgomery, Alabama.

3. Data Reduction

The preliminary reduction of the raw data is presented in Figs. II-14 and II-15. The effect of inadequate thermal control on Flight 737P shows in the enhanced noise for times later than 0900. These problems were at least partially overcome in Flight 738P but loss of the engineering data precludes knowledge of the thermal history on this flight.

During the next few months we shall refine the reduction, invert the data in several different ways, and make comparisons with radiosonde data taken at various stations close to the flight path.